Available online at www.sciencedirect.com
SCIENCE DIRECT®
Journal of Power Sources 138 (2004) 199–204
JOURNAL OF POWER SOURCES
www.elsevier.com/locate/jpowsour

Short communication

# A dynamic model for a stand-alone PEM fuel cell power plant for residential applications

M.Y. El-Sharkh, A. Rahman*, M.S. Alam, P.C. Byrne, A.A. Sakla, T. Thomas

*Department of Electrical of Computer Engineering, University of South Alabama Mobile, AL 36688-0002, USA*

Received 25 May 2004; accepted 20 June 2004
Available online 13 August 2004

**Abstract**

A dynamic electrochemical simulation model of a grid independent proton exchange membrane (PEM) fuel cell power plant is presented. The model includes the methanol reformer, the PEM stack, and the power conditioning unit. The model is then used to predict the output voltage and study the transient response of a PEM power plant when subjected to rapid changes in a residential load connected to it. The results show the fast response capabilities of the PEM power plant in following changes in the load.


*Keywords:* Fuel cell; PEM fuel cell; Electrochemical model; Dynamic model

## 1. Introduction

The ever increasing demand for electrical energy and the intense competition between electric companies in the new electric utility market has intensified research in alternative sources of electrical energy that are reliable and cost effective. The fuel cell, as a renewable energy source, is considered one of the most promising sources of electric power. Fuel cells are not only characterized by higher efficiency than conventional power plants, but they are also environmentally clean, have extremely low emission of oxides of nitrogen and sulfur and have very low noise.

The fuel cell, in its elemental form, consumes hydrogen as a fuel and produces dc power. The commonly available fuel cells can be classified according to temperature, into low-temperature, medium-temperature, and high-temperature fuel cells [1]. The low-temperature fuel cells include the alkaline fuel cell (AFC), and solid polymer fuel cell (SPFC) or proton exchange membrane fuel cell (PEMFC). The medium-temperature class has the phosphoric acid fuel cell (PAFC). The high-temperature class has the molten-carbonate fuel cell (MCFC) and solid oxide fuel cell (SOFC).

The main components of the fuel cell system include the fuel processing unit or the reformer, the fuel cell stack and the power conditioning unit. In general, hydrogen fuel is produced by processing some hydrocarbon fuel, such as propane, natural gas, or methanol in the reformer. During fuel processing, carbon monoxide is produced. Reduction of carbon monoxide to acceptable levels is achieved by the water–gas shift reaction. The low-temperature and the medium-temperature fuel cells have external reformers for producing hydrogen. The high-temperature fuel cells process the hydrocarbon fuel internally due to the high working temperature. The output from a fuel cell is dc power. When a fuel cell power plant (FCPP) provides power to a residential load, or to the electrical grid, a power conditioning unit is needed. The power conditioning unit is simply a dc/dc converter used to raise the C output voltage, which is generally the dc bus voltage, followed by a single-phase or a three-phase dc/ac inverter. In grid-parallel operation mode, a transformer is needed because of the voltage difference between the FCPP output voltage and the grid voltage. Due to the low working temperature (80–100 °C) and fast start up, PEMFCs are the best candidate for residential and vehicular

* Corresponding author. Tel.: +1 251 460 6117; fax: +1 251 460 6028.
*E-mail address:* arahman@usouthal.edu (A. Rahman).

0378-7753/$ – see front matter © 2004 Elsevier B.V. All rights reserved.
doi:10.1016/j.jpowsour.2004.06.037

applications. The reasons behind selecting the PEM FCPP in this paper are: (a) fuel cell user groups publications indicated that for small residential applications, where major heating appliances are natural gas operated, a 5 kw unit is adequate. (b) A 5 kw commercial PEM FCPP is currently operational in the authors' lab.

Many models have been proposed to simulate the fuel cell in the literature. The basis of a model can be fluid dynamics, electrochemical reaction, heat transfer and thermal [2–10]. To study the transient response and load following ability of a PEM FCPP, this paper introduces an electrochemical model for a 5 kW fuel cell. The scheme incorporates the model for an external reformer to generate hydrogen from methanol.

The paper is organized as follows: Section II introduces a model for the fuel cell system. Load following tests of the model is presented in Section III. Section IV presents the conclusions.

## 2. Fuel cell system model

### 2.1. Fuel cell model

In [6], Padulles et al. introduced a model for the SOFC. This model can be modified to simulate the PEM FCPP as follows:

The proportional relationship of the flow of gas through a valve with its partial pressure can be stated as [6]:

$$\frac{q_{\mathrm{H_2}}}{p_{\mathrm{H_2}}} = \frac{k_{\mathrm{an}}}{\sqrt{M_{\mathrm{H_2}}}} = k_{\mathrm{H_2}} \tag{1}$$

and

$$\frac{q_{\mathrm{H_2O}}}{p_{\mathrm{H_2O}}} = \frac{k_{\mathrm{an}}}{\sqrt{M_{\mathrm{H_2O}}}} = k_{\mathrm{H_2O}} \tag{2}$$

where $q_{\mathrm{H_2}}$is molar flow of hydrogen (kmol s$^{-1}$), $q_{\mathrm{H_2O}}$ molar flow of water (kmol s$^{-1}$), $p_{\mathrm{H_2}}$ hydrogen partial pressure (atm), $p_{\mathrm{H_2O}}$ water partial pressure (atm), $k_{\mathrm{H_2}}$ hydrogen valve molar constant (kmol (atm s)$^{-1}$), $k_{\mathrm{H_2O}}$ water valve molar constant (kmol (atm s)$^{-1}$), $k_{\mathrm{an}}$ anode valve constant ($\sqrt{\mathrm{Kmol\,Kg}}$ (atm s)$^{-1}$), $M_{\mathrm{H_2}}$ molar mass of hydrogen (kg kmol$^{-1}$), $M_{\mathrm{H_2O}}$ molar mass of water (kg kmol$^{-1}$).

For hydrogen, the derivative of the partial pressure can be calculated using the perfect gas equation as follows [6]:

$$\frac{\mathrm{d}}{\mathrm{d}t}p_{\mathrm{H_2}} = \frac{\mathrm{RT}}{V_{\mathrm{an}}}(q^{\mathrm{in}}_{\mathrm{H_2}} - q^{\mathrm{out}}_{\mathrm{H_2}} - q^{r}_{\mathrm{H_2}}) \tag{3}$$

where $R$ is the universal gas constant ((l atm) (kmol K)$^{-1}$), $T$ absolute temperature (K), $V_{\mathrm{an}}$ volume of the anode (l), $q^{\mathrm{in}}_{\mathrm{H_2}}$ hydrogen input flow (kmol s$^{-1}$), $q^{\mathrm{out}}_{\mathrm{H_2}}$ hydrogen output flow (kmol s$^{-1}$), $q^{r}_{\mathrm{H_2}}$ hydrogen flow that reacts (kmol s$^{-1}$).

The relationship between the hydrogen flow and the stack current can be written as:

$$q^{r}_{\mathrm{H_2}} = \frac{N_o I}{2F} = 2k_r I \tag{4}$$

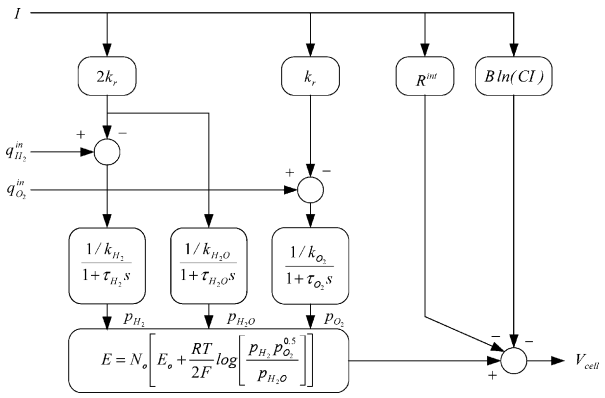


Fig. 1. The PEM fuel cell model.

where is $N_o$: number of series fuel cells in the stack, $I$ stack current (A), $F$ Faraday's constant (C kmol$^{-1}$), $k_r$ modeling constant (kmol (s A)$^{-1}$).

Using equation (4), Eq. (3) can be rewritten in the $s$ domain as:

$$p_{\mathrm{H_2}} = \frac{1/k_{\mathrm{H_2}}}{1+\tau_{\mathrm{H_2}}s}(q^{\mathrm{in}}_{\mathrm{H_2}} - 2k_r I) \tag{5}$$

where:

$$\tau_{\mathrm{H_2}} = \frac{V_{\mathrm{an}}}{k_{\mathrm{H_2}}\mathrm{RT}} \quad \mathrm{s} \tag{6}$$

Using Eq. (5), the equations for the partial pressures of water $p_{\mathrm{H_2O}}$, and oxygen $p_{\mathrm{O_2}}$ can also be derived.

In [7] and [8], the authors introduce a model that describes the polarization curves for the PEM fuel cell where the fuel cell voltage is the sum of three terms, the Nernst instantaneous voltage $E$ in terms of gas molarities, activation over voltage $\eta_{\mathrm{act}}$, and ohmic over voltage $\eta_{\mathrm{ohmic}}$. In mathematical form, polarization curves can be expressed by the equation:

$$V_{\mathrm{cell}} = E + \eta_{\mathrm{act}} + \eta_{\mathrm{ohmic}} \tag{7}$$

where $\eta_{\mathrm{act}}$ is a function of the oxygen concentration $C_{O_2}$ and stack current $I$ (A), and $\eta_{\mathrm{ohmic}}$ is a function of the stack current and the stack internal resistance $R^{\mathrm{int}}$ (Ω). Assuming constant temperature and oxygen concentration, Eq. (7) can be rewritten as [8]:

$$V_{\mathrm{cell}} = E - B\ln(CI) - R^{\mathrm{int}}I \tag{8}$$

where constants, $B = 0.04777$ V and $C = 0.0136$ A$^{-1}$ [7]. The Nernst voltage in terms of gas molarities can be written as [6]:

$$E = N_o\left[E_o + \frac{\mathrm{RT}}{2F}log\left[\frac{p_{\mathrm{H_2}}p^{0.5}_{\mathrm{O_2}}}{p_{\mathrm{H_2O}}}\right]\right] \tag{9}$$

where $E_o$ is the open cell voltage ($V$) and $R$ is the universal gas constant (J (kmol K)$^{-1}$.

Using Eqs. (5), (8) and (9) the fuel cell model can be drawn as in Fig. 1 [6].

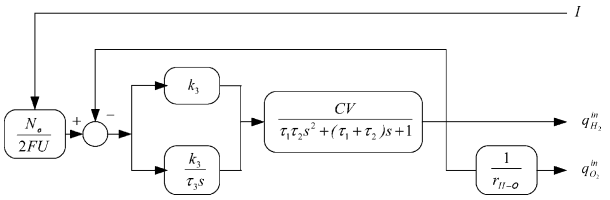


Fig. 2. The reformer and the reformer controller model.

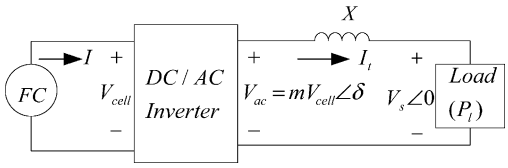


Fig. 3. Fuel cell, inverter and load connection diagram.

### 2.2. Reformer model

In [9] the author introduced a simple model of a reformer that generates hydrogen through reforming methanol. The model is a second order transfer function. The mathematical form of the model can be written as follows:

$$\frac{q_{H_2}}{q_{\text{methanol}}} = \frac{CV}{\tau_1\tau_2 s^2 + (\tau_1+\tau_2)s + 1} \tag{10}$$

where $q_{\text{methanol}}$ is methanol flow rate (kmol s$^{-1}$), $CV$ conversion factor (kmol of hydrogen kmol$^{-1}$ of methanol), $\tau_1$,$\tau_2$ time constants (s).

To control hydrogen flow according to the output power from the fuel cell, a feedback from the stack current is considered. The relationship between the required hydrogen and the increase in the stack current can be written as:

$$q^{\text{req}}_{H_2} = \frac{N_o I}{2\text{FU}} \tag{11}$$

where $q^{\text{req}}_{H_2}$ is amount of hydrogen flow required to meet the load change (kmol s$^{-1}$), $U$ Utilization rate.

The amount of hydrogen required to meet the load change can be used to control the methanol flow rate [9]:

$$q_{\text{methanol}} = \left(k_3 + \frac{k_3}{\tau_3 s}\right)\left(\frac{N_o I}{2\text{FU}} - q^{\text{in}}_{H_2}\right) \tag{12}$$

where $k_3$ is the PI gain and $\tau_3$ is the time constant of the PI controller. A proportional integral (PI) controller is used to control the flow rate of methanol in the reformer [9]. The oxygen flow is considered using the hydrogen, oxygen flow ratio $r_{\text{h–o}}$. The transfer function of the controller with the current feedback is given in Eq. (12). The reformer and the reformer controller are illustrated in Fig. 2.

### 2.3. The power conditioning unit model

The power conditioning unit is used to convert dc output voltage to ac. As mentioned before, the power conditioning unit includes a dc/dc converter to raise dc output voltage to dc bus voltage, followed by a dc/ac inverter to convert dc bus voltage to ac. In this paper, only a simple model of a dc/ac inverter is considered for the following reasons: the dynamic time constant of inverters is of the order of microseconds or at the most milliseconds. The time constants for the reformer and stack are of the order of seconds. Hence, including the inverter time constant will have negligible effect on the time response accuracy. On the other hand, it complicates the system model. All commercial FCPPs have to conform to IEEE standard #P-1547, which guarantees the ripples in the FCPP's output voltage to be within commercially acceptable limits. A simple model of the inverter is given in [10], where output voltage and output power are controlled using the inverter modulation index and the phase angle $\delta$ of the ac voltage, $V_{\text{ac}}$. Considering the fuel cell as a source, the inverter and load connection is shown in Fig. 3. The output voltage and the output power as a function of the modulation index and the phase angle can be written as:

$$V_{\text{ac}} = mV_{\text{cell}}\angle\delta \tag{13}$$

$$P_{\text{ac}} = \frac{mV_{\text{cell}}V_s}{X}\sin(\delta) \tag{14}$$

$$I_t = \frac{P_l}{(V_{\text{s}}\cos(\theta))} \tag{15}$$

$$I = mI_{\text{t}}\cos(\theta+\delta) \tag{16}$$

where: $V_{\text{ac}}$ is ac output voltage of the inverter (V), $m$ inverter modulation index, $\delta$: phase angle of the ac voltage $mV_{\text{cell}}$ (rad), $P_{\text{ac}}$ ac output power from the inverter (W), $V_{\text{s}}$ load terminal voltage (V), $X$ reactance of the line connecting the fuel cell and the load (Ω), $I_{\text{t}}$ load current (A), $\theta$ load phase angle (rad), $P_l$ load power (W).

As mentioned before, the modulation index is used to control the magnitude of the ac output voltage, which in turn controls the amount of reactive power flow to the load. The phase angle is used to control the active power flow from the inverter to the load. The voltage at load terminals is considered constant. PI controllers are used to control the modulation index and the phase angle feedback signals to the inverter. The transfer function of the modulation index and the phase shift are given in Eqs. (15) and (16).

$$m = \frac{k_5 + k_6 s}{s}(V_{\text{r}} - V_{\text{ac}}) \tag{15}$$

$$\delta = \frac{k_7 + k_8 s}{s}(P_{\text{r}} - P_{\text{ac}} + P_l) \tag{16}$$

where $k_5$, $k_6$, $k_7$, and $k_8$ are constants, $V_{\text{r}}$ is the reference voltage signal, $P_{\text{r}}$ is the reference power signal, and $P_{\text{l}}$ represents the load power. The block diagram of the inverter with the PI controllers is illustrated in Fig. 4.

The current feedback signal in Fig. 1 and Fig. 2, is calculated from the load information and the ac output voltage. Due to the assumed grid-independent operation the transformer model is not included.

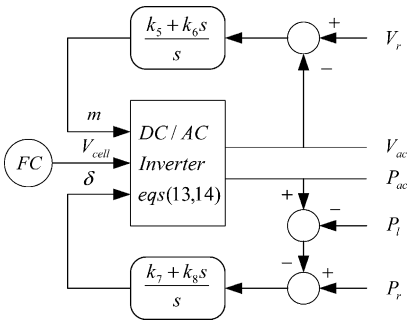


Fig. 4. The dc/ac inverter model.

## 3. Tests and Results

The models in Figs. 1, 2, and 4 are connected in cascade to form a complete model for the PEM fuel cell system.

The PEM FCPP we currently have in the lab, as well as commercial FCPPs, need at least an hour to start from cold to build up the reformer and stack temperatures. A minimum load value (critical load) has to be maintained all the time during FCPP operation. Decreasing the load below the critical load value will put the FCPP in a sleep or dormant mode, where a small amount of fuel is used to maintain the reformer and stack temperatures at operating levels. In the following test cases, the FCPP is assumed to be in the active mode and the initial active and reactive output powers are 0.8 and 0.6 p.u, respectively. The commercially available PEM FCPPs come equipped with storage batteries connected in parallel with the dc bus. These batteries serve as a short-period auxiliary power source to meet load demand that cannot be met by the FCPP, particularly during transient periods. Choosing the control system parameters affects the system performance. For example, increasing the gain of the PI controller that controls the modulation index makes the voltage less sensitive to load variations. Testing the proposed model indicates that the reformer and the reformer controller parameters have a large effect on the FCPP time response. The reformer parameters affect the reformer's damping factor. Choosing a damping factor of 1.0 for the uncontrolled reformer (open loop) will ensure that no unrealistic overshoot occurs [9]. This will yield $\tau_1 = \tau_2$. For maintaining stability and reasonable fuel processor dynamics of the controlled reformer, the controller parameters are chosen to ensure a damping factor of 0.707 [9]. With this assumption, the PI controller time constant $\tau_3$ is equal to $\tau_1$ and $k_3$ is equal to $(2CV)^{-1}$. The model parameters are given in Table 1.

Table 1
Model Parameters

| | |
|---|---|
| Stack Temperature, (K) | 343 |
| Faraday's constant, $F$ (C kmol$^{-1}$) | 96484600 |
| Universal gas constant, $R$ (J kmol$^{-1}$ K) | 8314.47 |
| No load voltage, $E_o$, (V) | 0.6 |
| Number of cells, $N_o$ | 88 |
| $K_r$ constant = $N_o/4F$ (kmol s$^{-1}$ A) | $0.996 \times 10^{-6}$ |
| Utilization factor, $U$ | 0.8 |
| Hydrogen valve constant, $K_{H2}$ (kmol s$^{-1}$ atm) | $4.22 \times 10^{-5}$ |
| Water valve constant, $k_{H_2O}$ (kmol s$^{-1}$ atm) | $7.716 \times 10^{-6}$ |
| Oxygen valve constant, $k_{O_2}$ (kmol s$^{-1}$ atm) | $2.11 \times 10^{-5}$ |
| Hydrogen time constant, $\tau_{H_2}$ (s) | 3.37 |
| Water time constant, $\tau_{H_2O}$ (s) | 18.418 |
| Oxygen time constant, $\tau_{O_2}$ (s) | 6.74 |
| Reformer time constant, $\tau_1$ (s) | 2 |
| Reformer time constant,$\tau_2$ (s) | 2 |
| Conversion Factor, $CV$ | 2 |
| Activation voltage constant, $B$ (A$^{-1}$) | 0.04777 |
| Activation voltage constant, $C$ (V) | 0.0136 |
| Stack internal resistance, $R^{int}$ (Ω) | 0.00303 |
| Line reactance, $X$ (Ω) | 0.05 |
| PI gain constants $k_5$, $k_6$ | 10 |
| Voltage reference signal, $V_r$ (p.u) | 1.0 |
| Methane reference signal, $Q_{methref}$ (kmol s$^{-1}$) | 0.000015 |
| Hydrogen-oxygen flow ratio, $r_{h-o}$ | 1.168 |

### 3.1. Case1

The FCPP model is tested with step changes in the load as shown in Fig. 5. These abrupt changes in active power are for testing the dynamic response of the system, and do not necessarily represent changes in a residential load. The change of the current, the voltage, the output power, and the flow rate of hydrogen and methanol are illustrated in Figs. 6–10. The

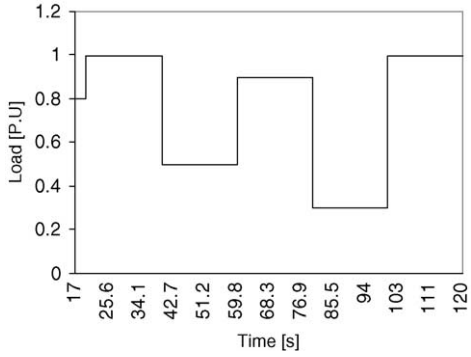


Fig. 5. Load step changes.

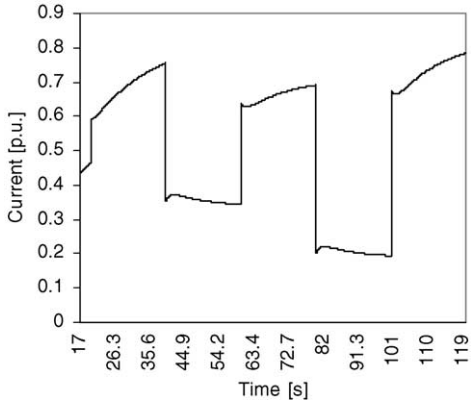


Fig. 6. Fuel cell dc output current.

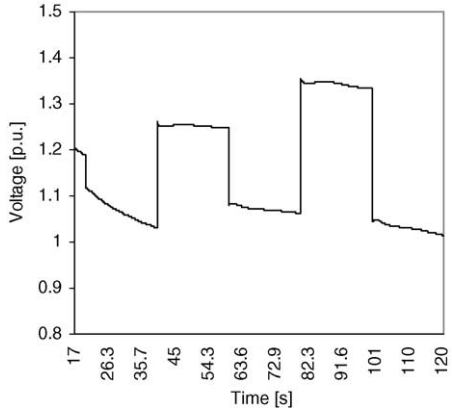


Fig. 7. Fuel cell dc output voltage.

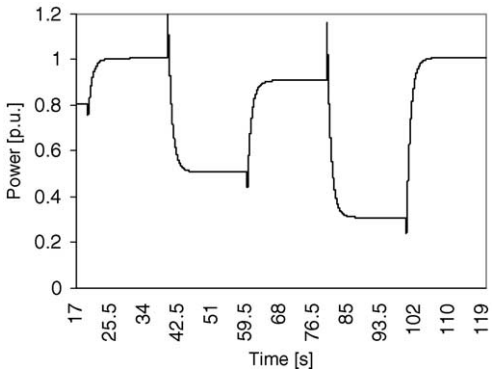


Fig. 8. ac output power.

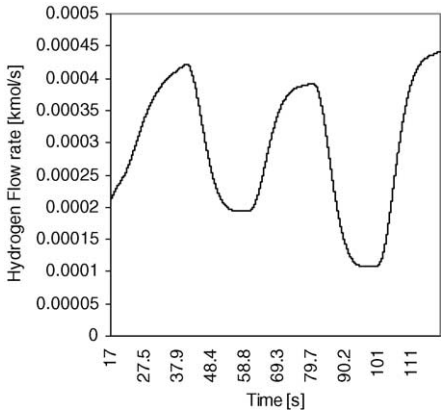


Fig. 9. Hydrogen flow rate.

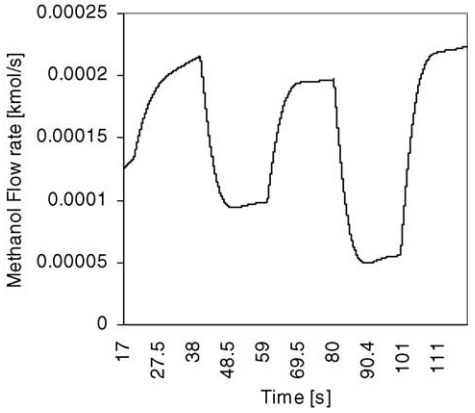


Fig. 10. Methanol flow rate.

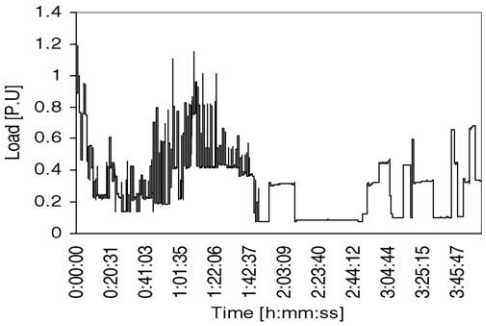


Fig. 11. Residential load profile for single circuit.

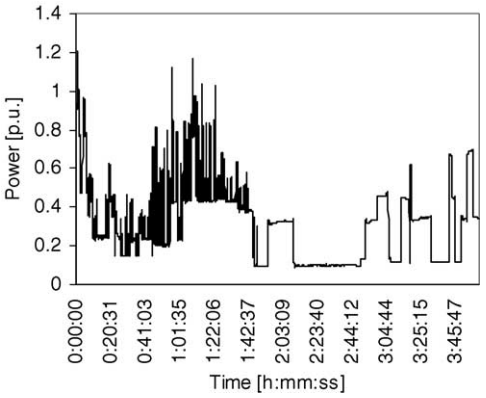


Fig. 12. ac output power.

time interval 0 to 17 s is not shown in the plots because it represents the dormant state of the FCPP. From these figures, it is evident that the increase in the load increases the feedback current, which in turn decreases the output voltage of the fuel cell. The increase in the current increases the methanol flow rate and the hydrogen flow rate to increase power flow from the cell to the load. As seen in the ac output power curve, the output power has a time delay in following the load power. This is due to the reformer and the fuel cell time constants.Case 2In this test case, the model is tested using an actual residential load profile. A load profile for a 2500 sq. ft. house with all electric appliances occupied by two adults and four children is used. Due to the limited output power of the fuel cell (5 kW), only one 120 V circuit of the house is considered. The active power load profile for a 4 h period with a 15 s sampling interval is shown in Fig. 11. The power and voltage bases are 5 kW and 120 V, respectively.

The purpose of this test is to check the load-following characteristics of the FCPP. The output power, current and voltage curves of the fuel cell are shown in Figs. 12–14.

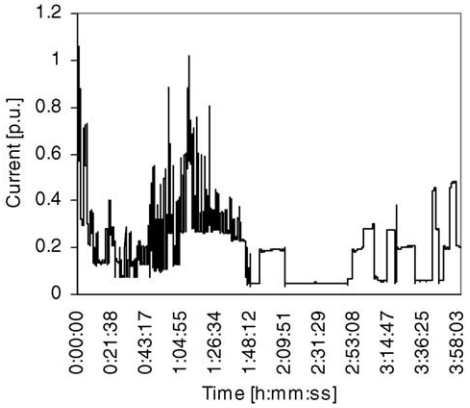


Fig. 13. Fuel cell dc output current.

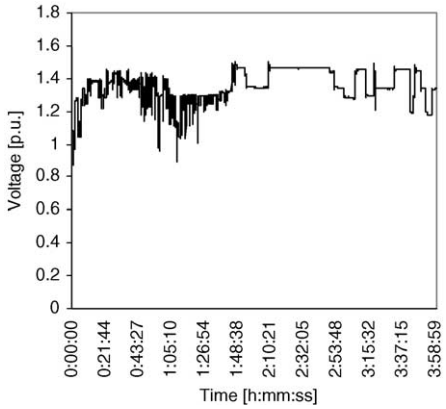


Fig. 14. Fuel Cell dc output voltage.

Comparison of Figs. 11 and 12 indicates that the FCPP demonstrates rapid response to residential load changes and exhibit good load-following capabilities.

## 4. Conclusions

This paper introduces a dynamic model for a 5 kW PEM fuel cell system. The proposed dynamic model includes the fuel cell model, the gas reformer model, and the power conditioning unit. To study the time response of the fuel cell, the proposed model has been tested with step increase and decrease of the electric load. The obtained results show a fast response of the fuel cell to load changes. To check the load-following characteristics, the proposed model has been tested using a typical residential load for a period of 4 h. The model showes a high degree of conformity.

## Acknowledgment

This research was supported by a grant from the Department of Energy (DE-FG02-02ER63376)

## References

[1] M.A. Laughton, Fuel cells, Power Eng. J., 2002, 37–47.
[2] U.M. Sukkee, C.Y. Wang, K.S. Chen, K.S. Chen, Computational dynamics modeling of proton exchange membrane fuel cell, J. Power Electrochem. Soc. 147 (2000) 12.
[3] D. Singh, D.M. Lu, N. Djilali, A two-dimension analysis of mass transport in proton exchange membrane fuel cells, Int. J. Eng Sci. 37 (1999) 431–452.
[4] S. Dutta, S. Shimpalee, J.W. Van Zee, Numerical prediction of mass-exchange between cathode and anode channels in PEM fuel cell, International, J. Heat Mass Transfer, 44, 2001.
[5] J.C. Amphlett, R.F. Mann, B.A. Peppley, P.R. Roberge, A. Rodrigues, A model predicting transient response of proton exchange membrane fuel cells, J. Power Sources 61 (1996) 183–188.
[6] J. Padulles, G.W. Ault, J.R. McDonald, An integrated SOFC plant dynamic model for power systems simulation, J. Power Sources 86 (2000) 495–500.
[7] J.C. Amphlett, R.M. Baumert, R.F. Mann, B.A. Peppley, P.R. Roberge, A. Rodrigues, Parametric modeling of the performance of a 5-kw proton exchange membrane fuel cell stack, J. Power Sources 49 (1994) 349–356.
[8] J. Hamelin, K. Agbossou, A. Laperriere, F. Laurencelle, T.K. Bose, Dynamic behavior of a PEM fuel cell stack for stationary applications, Int. J. Hydrogen Energy 26 (2001) 625–629.
[9] K.-H. Hauer, Analysis tool for fuel cell vehicle hardware and software (controls) with an application to fuel economy comparisons of alternative system designs, Ph.D. dissertation, Dept. Transportation Technology and Policy, University of California Davis, 2001.
[10] C.J. Hatziadoniu, A.A. Lobo, F. Pourboghrat, M. Daneshdoost, A simplified dynamic model of grid-connected fuel-cell generators, IEEE Trans. Power Delivery 17 (2002) 2.